13th Australasian Fluid Mechanics Conference
Monash University, Melbourne, Australia
13-18 December 1998

LARGE-EDDY SIMULATION OF TURBULENT PIPE FLOW ON SEMI-STRUCTURED GRIDS

Stefan SCHMIDT, Leiping XUE and Frank THIELE

Hermann-Föttinger-Institut für Strömungsmechanik
Technische Universität Berlin, GERMANY

ABSTRACT

Large-Eddy Simulations (LES) of a fully developed turbulent pipe flow were carried out based on a semi-structured multiblock finite-volume method. For calculating complex geometries, these grids provide much of the flexibility of unstructured meshes while offering reasonable advantages in grid generation with less computational effort. The aim of this work is to investigate the influence of different subgrid-scale models, the need of higher order convection approximation and the impact of energy conservation on the use of semi-structured grids. As a reference, a Direct Numerical Simulation (DNS) at a Reynolds number of $Re_\tau = 360$ based on the friction velocity u_τ and the pipe diameter D was performed.

INTRODUCTION

In the past, most of the numerical simulations (DNS, LES) carried out were based on single-block cartesian grids. One of the first investigations in this respect is the well known Direct Numerical Simulation (DNS) of a turbulent plane channel flow by Kim et al. (1987). The application to pipe flows was performed by Eggels et al. (1994) at Reynolds number $Re_\tau = 360$ using an axisymmetric coordinate frame. The grid used was highly stretched normal to the wall (r) and in circumferential direction (θ). Therefore, the control volumes had large aspect ratios from 4.7 at the pipe wall to 140 at the centreline of the pipe.

To calculate flows within more complex geometries cartesian grids are not suitable, as structured grids which are refined in certain areas of interest remain condensed also in parts of the domain where no refinement is needed. A possibility to overcome this restriction is the use of so-called semi-structured multiblock grids. They allow for more flexibility in grid generation, since semi-structured grids can be refined nearly anywhere while retaining the logical blockwise structure of single-block grids. Furthermore, as compared to unstructured grids, a higher numerical accuracy can be achieved at a lower computational cost. We propose an efficient numerical scheme based on the approximation of the incompressible Navier-Stokes equations on semi-structured grids with higher order discretisation of the convective fluxes. The standard subgrid-scale model (Smagorinsky, 1963) as well as dynamic models (Germano, 1990; Lilly, 1992; Davidson, 1997) were used to capture complex flow dynamics including phenomena such as transition and recirculation areas.

NUMERICAL METHOD

In the present study, an improved 3d multiblock finite-volume method developed by Xue (1998) is introduced, which allows to handle complex geometries in a more general way. The procedure is of second order accuracy in time and space. In addition, convective terms are discretized by a compact 4th order central differencing scheme:

$$\phi_e = \frac{\phi^P + \phi^E}{2} + \frac{\Delta\phi^P - \Delta\phi^E}{8} \qquad (1)$$

$$\Delta\phi^i = \left.\frac{\partial\phi}{\partial x_j}\right|^i \Delta x_j \quad ; \quad \Delta x_j = x_j^E - x_j^P$$

At block interfaces, the 4th order scheme retains its accuracy because the scheme is based on the values next to the boundary and their gradients. At physical boundaries, the standard central-differencing scheme is used. However, the integration scheme still uses the second order midpoint rule to keep the discretization molecule bounded.

SUBGRID-SCALE MODEL

In LES, the effect of large turbulent scales are explicitly resolved while the small scales, which behave in an universal isotropic way, are modelled by a subgrid-scale model. In this study, the Smagorinsky model is used

$$\tau_{ij}^{sgs} = -2\,\nu_T\,\overline{S}_{ij} \quad ; \quad \nu_T = (C_S\overline{\Delta})^2\sqrt{2\,\overline{S}_{ij}\,\overline{S}_{ij}}$$

where ν_T denotes the eddy-viscosity, $\overline{\Delta} = (\Delta x \Delta y \Delta z)^{1/3}$ and $\overline{S}_{ij} = 0.5(\overline{u}_{i,j} + \overline{u}_{j,i})$ is the strain rate. An additional wall damping function $C_S = C_{S_0}(1-\exp^{(y^+/A^+)^a})^b$ (A^+=25, a=3.0, b=0.5) is used to give the correct near wall behaviour of the viscosity. Since this model is based on equilibrium of production and dissipation and requires a parameter C_S which strongly depends on the shear rate, it fails to react to local non-equilibrium states. The dynamic procedure (Germano, 1991) evaluates the Leonard-stresses $\mathcal{L}_{ij} = \widetilde{\overline{u}_i\overline{u}_j} - \widetilde{\overline{u}}_i\widetilde{\overline{u}}_j$ via an explicit filtering, denoted by $\widetilde{(.)}$, which can be used to calculate a parameter C as a function of time and space. A least-square procedure (Lilly, 1992) leads to the dynamic Germano-Lilly Model.

$$\begin{aligned} C &= -\frac{\mathcal{L}_{ij}\, M_{ij}}{2\, M_{ij}\, M_{ij}} \\ M_{ij} &= \widetilde{\overline{\Delta}}\, |\widetilde{\overline{S}}|\, \widetilde{\overline{S}}_{ij} - \overline{\Delta}\, \widetilde{|\overline{S}|\overline{S}_{ij}} \end{aligned} \qquad (2)$$

This formulation avoids the singularity in the denominator. However, large parameter variations still remain. Davidson (1997) suggests an alternative approach by solving a transport equation for the subgrid kinetic energy k_{sgs}.

$$\begin{aligned} \tau_{ij}^{sgs} &= -2\,\overline{\Delta}\, k_{sgs}^{\frac{1}{2}}\, \overline{S}_{ij} \quad ; \quad K = \widetilde{k_{sgs}} + \frac{1}{2}\mathcal{L}_{ii} \\ M_{ij} &= \widetilde{\overline{\Delta}}\, K^{\frac{1}{2}}\, \widetilde{\overline{S}}_{ij} - \overline{\Delta}\, \widetilde{k_{sgs}^{\frac{1}{2}}\, \overline{S}_{ij}} \end{aligned}$$

The effect of backscatter, i.e. the reverse transport of kinetic energy from small to large scales, is taken into account in a different way as compared to the standard dynamic model. The parameter C is calculated using Eq.(2), influencing only the production $P_{k_{sgs}} = -\tau_{ij}^{sgs}\overline{u}_{i,j}$. A negative production therefore leads to a decrease of k_{sgs} and hence of ν_T. For stability reasons, a global average of $<C>_{xyz}$ is used for the momentum equations. Finally, this model contains a parameter C_* which is computed assuming that the r.h.s. of the k_{sgs} and K equation are equal:

$$C_* = \left(P_{k_{sgs}} - \widetilde{P_{k_{sgs}}} + \frac{1}{\overline{\Delta}} C_*\, \widetilde{k_{sgs}^{\frac{3}{2}}}\right) \frac{\widetilde{\overline{\Delta}}}{K^{\frac{3}{2}}}$$

with $0 < C_* < 10$. The important feature is that this model adapts itself to the local turbulence structure as well as to variations of the grid size; the influence of the model vanishes in case of DNS and laminar flow.

BOUNDARY AND INITIAL CONDITIONS

In accordance to prior investigations, a Reynolds number of $Re_\tau = 360$ based on the friction velocity u_τ and the pipe diameter D was chosen to validate the numerical method. The geometry of the testcase is shown in Figure 1, where L is the length of the pipe, which is chosen to be $L = 5D$ to resolve all relevant turbulent scales.

Boundary Conditions

At the wall, a no-slip condition is imposed. In the streamwise direction (z), periodic boundaries are applied. The flow is driven by a pressure difference which is obtained from the momentum balance between the pressure force and the reacting force of the wall shear stress. Since natural variations of the total mass flux through the whole flow domain appear during the simulation, an adaptive control procedure is added which guarantees non-varying values of the friction velocity and therefore of the Re-number Re_τ.

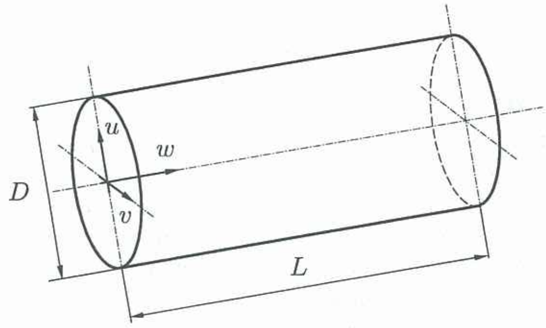

Figure 1: Sketch of the flow geometry.

Initial Conditions

The Large-Eddy Simulations were initialised with a superposition of a laminar profile and an additional random noise of the order of 20% of the mean velocity. In case of the DNS, a sinussoidal wave in the homogeneous direction with an amplitude of half of the mean velocity was additionally added. After a period of $T_{Init} = 150s$ the flow reached a fully turbulent state.

NUMERICAL GRID

The grids of the different test cases are shown in Figure 2. In the core region, a H-type grid is used to avoid singularities at the centreline of the pipe, while an O-type grid is used in the near wall region, allowing for easy refinement.

For the LES, different grids with unstructured block interfaces were used. The coarse LES (LES 10x10) and the DNS (DNS 30x30) use only structured block interfaces, while the other two LES cases use unstructured block interfaces in all directions (LES 15x20) and only in the mean flow direction (LES 20x20), respectively. Details of the numerical grids can be found in Table 1.

CALCULATION AND RESULTS

The DNS provides detailed data for the validation of the numerical method and is used to generate velocity profiles for non-periodic geometries. The LES calculations were performed at the same Re-number with

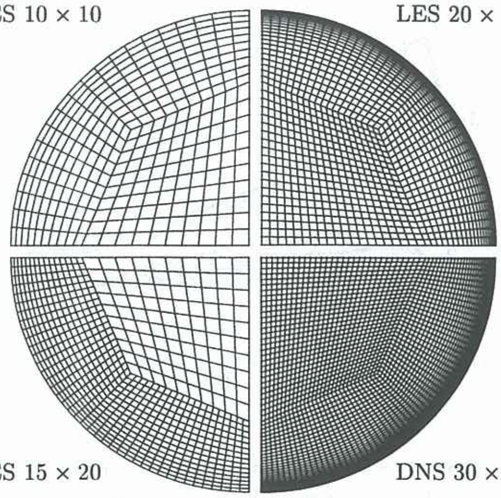

Figure 2: Numerical grids in the cross-section of the pipe.

	LES			DNS
Case	10×10	15×20	20×20	30×30
Nodes	60'000	260'000	400'000	2'700'000
Blocks	12	12	12	60
PEs	12	9	10	60
core region: 4 blocks / wall region: 8 blocks				
N_x	10/ 10	10/ 15	20/ 20	30/ 30
N_y	10/ 10	10/ 20	20/ 20	30/ 30
N_z	50/ 50	50/100	50/100	250/250
grid spacing in wallunits: min/max				
core region				
Δx^+	8.9/12.6	8.9/12.6	4.5/ 6.3	3.0/ 4.2
Δy^+	8.9/12.6	8.9/12.6	4.5/ 6.3	3.0/ 4.2
Δz^+	36/ 36	18/ 36	18/ 36	7.2/ 7.2
wall region				
Δx^+	3.8/ 6.5	2.5/ 4.3	0.8/ 4.5	0.5/ 3.0
Δy^+	8.9/14.1	4.5/ 7.1	4.5/ 7.1	3.0/ 4.7
Δz^+	36/ 36	18/ 36	18/ 36	7.2/ 7.2

Table 1: Overview of numerical grids.

different grid resolutions and topologies to investigate the grid dependency of the flow properties.

The simulations were carried out on a massively parallel computer Cray T3E-900 and the load balance was adapted to minimize latency between the computational nodes. The code achieved 57.5 MFlops per node on 60 Processing Elements (PE's) with a maximum of 6% PVM-overhead which results in an overall performance of 3.5 GFlops. The simulation time extended over 24'000 time steps with a physical time step of $\Delta t = 0.01s$. Averages of the velocities were taken starting from $T = 200s$ at $\Delta T = 0.1s$.

Mean flow properties

The averaged mean velocity profiles are shown in Figure 3 together with recent experimental data by Toonder (1995). The present DNS data nearly match those

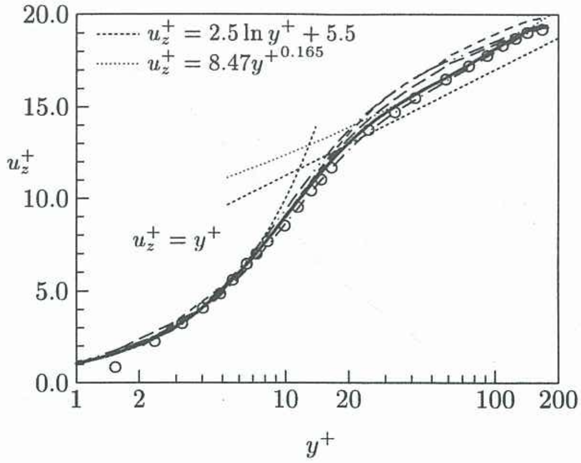

Figure 3: Axial mean velocity distribution normalized by friction velocity: present DNS data (——) compared with data (–·–·) from Eggels (1994); LES 10x10 (- - - -), LES 15x20 (– – –), LES 20x20 (–··–); LDA measurements (○) carried out by Toonder (1995); the dotted line represents the universal law of the wall.

obtained by Eggels. However, they fail to conform to the logarithmic velocity distribution. The LES results show good agreement near the wall ($y^+ \leq 10$) but slightly overshoot the DNS results in the core region ($y^+ \geq 30$). Comparing the results of case LES 10x10 and LES 15x20 shows that an increase of grid points in the wall region leads to better results also in the core region. The general overprediction of the universal law of the wall is due to a wake region which is typical for pipe flows. Zagarola & Perry (1997) found that for small Re-numbers a power law would be preferable to a log law. A power law which best suits the present DNS data (DNS 30x30) can be evaluated through a least-square procedure: $u^+ = C\, y^{+\,\gamma}$ with $C = 8.47, \gamma = 0.165$.

In Figure 4, the results of different subgrid-scale models are shown for testcase LES 10x10. The dynamic model and the one-equation dynamic model capture the slope of the experimental data but overpredict them in the core of the pipe. The damped Smagorinsky model cannot follow the gradient and remains beneath the correct velocity distribution.

Turbulence Intensities

The turbulence intensities of both DNS and LES are compared with numerical data (Eggels, 1994) and experimental data (Toonder, 1995). While the DNS resolves all turbulent scales, the Reynolds stresses consist only of $\overline{u_i' u_j'}$. In case of the LES, those terms have to be assembled from resolved stresses $\overline{u_i'' u_j''}$ and modelled stresses τ_{ij}^{sgs}. Those subgrid stresses decrease with higher grid resolution and vanish in case of DNS. The Reynolds stresses of the present DNS are in fairly good agreement with the numerical data and the LDA measurements (Fig. 5). The peak of the

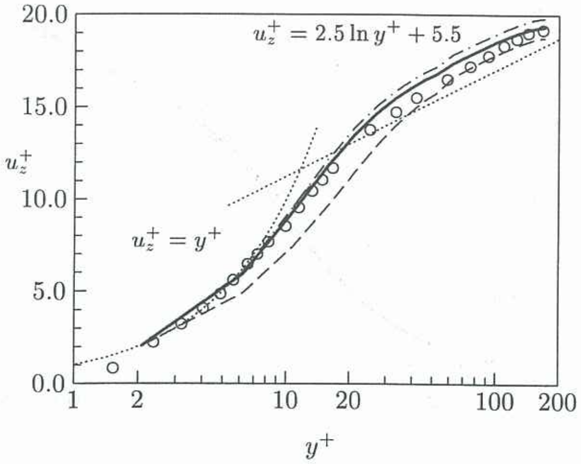

Figure 4: Axial mean velocity distribution normalized by friction velocity of LES 10x10 with different sgs-models; Smagorinsky Model with Van Driest-Damping (– – –), Dynamic Model (– · – ·), Dynamic-One-Equation Model (——); LDA measurements (o) carried out by Toonder (1995); the dotted line represents the universal law of the wall.

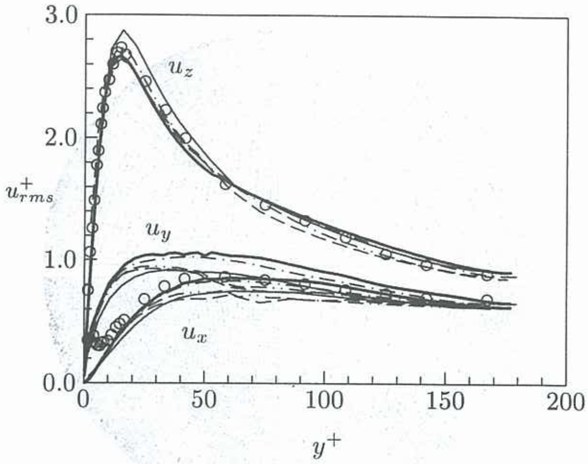

Figure 5: rms-values of velocity normalized by friction velocity: present DNS data (——) compared with data (– · – ·) from Eggels (1994); LES 10x10 (——), LES 15x20 (– – –), LES 20x20 (– · · –); LDA measurements (o) carried out by Toonder (1995).

mean normal stress $u^+_{z_{rms}}$ is slightly underestimated while the other stresses are captured quite well. From the coarse grid LES results it can be seen that the profiles of the normal stresses u_x^+ and u_y^+ are too small and u_z^+ has its peak value too far off the wall while being generally overpredicited.

CONCLUSION

Large-Eddy Simulation and Direct Numerical Simulation of a turbulent pipe flow were performed on semi-structured grids using a multiblock finite-volume method. The numerical simulations demonstrate that good results can be obtained with this finite-volume method of second order accuracy in time and space. Due to the use of semi-structured meshes the numerical method saves grid points in areas of lesser physical importance, which are in most cases over 50% of the whole flow domain, and offers the possibility to refine the grid locally to resolve unsteady flow patterns in time and space. As long as the grid resolution is sufficiently high to resolve the large, energy containing motion of the flow, good results can be achieved. Before starting the simulation it has to be checked, which parts of the computational domain require high resolution grids to capture all relevant turbulent structures.

ACKNOWLEDGEMENTS

This research was partly sponsored by the German Ministry of Education and Research (BMBF) under the umbrella of the MEGAFLOW project (Grants No. 20A9501F and 20A9505H) and the Deutsche Forschungsgemeinschaft (DFG-SFB 557).

REFERENCES

DAVIDSON, L., "Large Eddy Simulations: A dynamic one-equation subgrid model for three-dimensional recirculating flow", *11th Int. Symp. on Turbulent Shear Flow*, Grenoble, **3**, 26.1-26.6, 1997.

EGGELS, J.G.M., UNGER, F., WEISS, M.H., WESTERWEEL, J., ADRIAN, R.J., FRIEDRICH, R. and NIEUWSTADT, F.T.M., "Fully developed turbulent pipe flow: a comparison between direct numerical simulation and experiment", *J. Fluid Mech.*, **268**, 175-209, 1994.

GERMANO, M., PIOMELLI, U., MOIN, P. and CABOT, W.H., "A dynamic subgrid-scale eddy viscosity model", *Physics of Fluids*, **A3**, 1760-1765, 1991.

KIM, J., MOIN, P. and MOSER, R., "Turbulence statistics in fully developed channel flow at low Reynolds number", *J. Fluid Mech.*, **177**, 133-166, 1987.

LILLY, D.K., "A proposed modification of the Germano subgrid-scale closure method", *Physics of Fluids*, **A4**, 633-635, 1992.

SMAGORINSKY, J., "General circulation experiments with the primitive equations", *Monthly Weather Review*, **91**, 99-164, 1963.

TOONDER, J.DEN and NIEUWSTADT, F.T.M., "Reynolds number effects in a turbulent pipe flow for low to moderate Re", submitted to *Physics of Fluids*, 1995.

XUE, L., "Entwicklung eines effizienten parallelen Lösungsalgorithmus zur dreidimensionalen Simulation komplexer turbulenter Strömungen", *Dissertation*, Hermann-Föttinger-Institut für Strömungsmechanik, Technische Universität Berlin, 1998.

ZAGAROLA, M.V., PERRY, A.E. and SMITS, A.J., "Log laws or power laws: The scaling in the overlap region", *Physics of Fluids*, **9**, 2094-2100, 1997.